Journal of Applied Polymer Science

# Submicrometer-Sized Rubber Particles as "Craze-Bridge" for Toughening Polystyrene/High-Impact Polystyrene

**Li Dan Zhu,[1] Hong Yu Yang,[1] Gui Di Cai,[1] Chao Zhou,[1] Guang Feng Wu,[1] Ming Yao Zhang,[1] Guang Hui Gao,[1] Hui Xuan Zhang[1,2]**

[1]Engineering Research Center of Synthetic Resin and Special Fiber, Ministry of Education, Changchun University of Technology, Changchun 130012, China

[2]Changchun Institute of Applied Chemistry, Chinese Academy of Sciences, Changchun 130012, China

Correspondence to: G. H. Gao (E-mail: ghgao@mail.ccut.edu.cn)

**ABSTRACT:** Submicrometer core-shell polybutadiene-*graft*-polystyrene (PB-*g*-PS) copolymers were synthesized by emulsion grafting polymerization with 1,2-azobisisobutyronitrile as an initiator. Then, PB-*g*-PS copolymers were blended with high-impact polystyrene (HIPS) and PS to prepare HIPS/PS/PB-*g*-PS. It is generally accepted that PS could only be toughened by 1–3-$\mu$m rubber particles effectively. From the Izod impact test, however, the results showed that PS could be toughened effectively by submicrometer rubber particles (around 300 nm) in our study. Moreover, the impact strength of HIPS/PS/PB-*g*-PS is much higher than that of HIPS due to the synergism between submicrometer rubber particles and micrometer salami particles. Subsequently, the stress-whitening zones for HIPS, PS/PB-*g*-PS, and HIPS/PS/PB-*g*-PS were also observed in detail by transmission electron microscope. Based on mechanical properties and deformation morphologies, the deformation mechanism in the HIPS/PS/PB-*g*-PS blends was given as follows: crazes could be initiated from large rubber particles, passed through "craze-bridge" rubber particles, and ended to neighboring small one, which prevented excessively crazing to be form cracks, absorbed energy, and finally enhanced the toughness of PS. © 2012 Wiley Periodicals, Inc. J. Appl. Polym. Sci. 129: 224–229, 2013

**KEYWORDS:** blends; emulsion polymerization; polystyrene; resins

Received 6 July 2012; accepted 11 October 2012; published online 6 November 2012
**DOI: 10.1002/app.38716**

## INTRODUCTION

Polystyrene (PS) is a hard, brittle thermoplastics, and can only be applied after toughened by rubber particles. Generally, high-impact polystyrene (HIPS) is prepared by bulk or bulk-suspension polymerization of styrene containing dissolved polybutadiene (PB) rubbers, and the micrometer rubber particles with a "salami" structure in HIPS can be observed.[1,2] Moreover, in the recent years, there are some works about toughening PS or HIPS with different types of rubber particles.[3–5] It was reported that PS or HIPS could be toughened more efficiently with either 1–3-$\mu$m "salami" rubber particles[6–8] or an adequate combination of submicrometer rubber particles.[9–11]

Several principal mechanisms of rubber-toughened plastics have been reported, including multiple crazes, shear yielding, crazing with shear yielding, and cavitation. The primary deformation mechanism was multiple crazes for HIPS with micrometer "salami" rubber particles.[12,13] Besides, some researchers have reported that PS can be toughened efficiently by rubber particles with dual particle sizes. The way to absorb energy during the deformation process was crazing and cavitation induced by rubber particles.[10]

Another preparation method of PB-toughened PS was given as follows: the crosslinked PB rubber particles were grafted by PS shell via emulsion polymerization and then blended with PS to prepare PS/PB-*g*-PS.[14,15] In the previously reported work, it has been found that 1,2-azobisisobutyronitrile (AIBN) is a particularly poor initiator to promote the grafting reaction of styrene onto natural rubbers (NR).[16] This is believed to be the result of its inability to abstract hydrogen atoms from the NR backbone molecules. However, Huang and Sundberg[17–19] studied the grafting reaction of three vinyl monomers (styrene, benzyl methacrylate, and benzyl acrylate) onto PB rubber particles. They suggested that the grafting reaction initiated by AIBN could occur on the double bond. Moreover, the oil-soluble initiator was found to be efficient in generating reactive radicals in the monomer-swollen micelles or polymer particles in an emulsion system.[20]

In this work, submicrometer core-shell polybutadiene-*graft*-polystyrene (PB-*g*-PS) particles were synthesized via emulsion grafting polymerization by grafting styrene onto PB latex with AIBN as an oil-soluble initiator. Then, these PB-*g*-PS copolymers were blended

with HIPS to prepare HIPS/PB-*g*-PS blends. To balance the yield strength and impact strength of polymer blends, PS was introduced to obtain HIPS/PS/PB-*g*-PS. Then the Izod notched impact test and the tensile test were used to characterize the mechanical properties of samples. Moreover, the morphologies of core-shell particles dispersed in the PS and/or HIPS matrix were observed by transmission electron microscope (TEM). Subsequently, the stress-whitening zones for HIPS, PS/PB-*g*-PS, and HIPS/PS/PB-*g*-PS under the tensile condition were also investigated. Finally, the corresponding deformation mechanisms were extensively discussed based on mechanical properties and deformation morphologies.

## EXPERIMENTAL

### Materials

PS (GPPS525, $M_w$ = 225,000) was supplied from Panjin Petro Chemistry Company, China. PB latex with an average particle size of 314 nm was kindly supplied by Jilin Chemistry Company, China. Styrene was purified by washing with 5% sodium hydroxide solution to remove the inhibitor. AIBN (Aldrich Chemical) was re6crystallized by ethanol before using. A commercial HIPS, which contained around 7% rubber content with a density of 1.05 g/cm$^{-3}$, was obtained from Chevron Phillips Chemical Company.

### Preparation of PB-*g*-PS

Core-shell PB-*g*-PS copolymers were synthesized with an emulsion polymerization by grafting styrene onto PB latex particles. A fixed ratio of styrene to PB (60 : 40) was added into the reaction system. AIBN was selected as an oil-soluble initiator. The polymerization was performed in a 3-L flask under nitrogen at 70°C. The reaction medium was stirred at 300 rpm, and nitrogen gas was purged into the reactor throughout the reaction. The styrene monomer dissolved AIBN was added in a continuous feeding way to the reaction system in 3 h, and then the reaction was carried out for another 3 h. The antioxidant solution was added into the reactor after decreasing the temperature to 50°C, and the reaction was ended in 30 min. After reaction, the latex was coagulated in addition to the magnesium sulfate ($MgSO_4$) solution to yield loose aggregation of the particles. The aggregates were washed thoroughly with water and then dried at 50°C in the oven for 24 h.

### Grafting Degree of PB-*g*-PS Copolymers

The grafting degree (GD) was determined by extracting the ungrafted or free PS of 0.5 g grafting copolymers by 5 mL methyl ethyl ketone (a solvent for PS but not for PB-*g*-PS). After the methyl ethyl ketone solution of the dried grafting copolymer was shaken for 24 h at room temperature, the solution was centrifuged at 10,000 rpm in a GL-21M centrifugal machine for 30 min with a temperature of −5°C. The grafting degree (GD) and grafting efficiency (GE) were calculated by the following equation:

$$\text{Grafting Degree(GD)} = \frac{\text{weight of grafted polystyrene}}{\text{weight of polybutadiene}} \times 100\%$$

$$\text{Grafting Efficiency(GE)} = \frac{\text{weight of grafted monomer}}{\text{weight of fed monomer}} \times 100\%$$

### Blending and Molding Procedures

The HIPS/PS/PB-*g*-PS or PS/PB-*g*-PS blends were prepared by mixing HIPS, PS, and PB-*g*-PS copolymers in a twin-screw extruder. The temperature along the extruder was set as 190–200°C, and the rotation speed of the screw was 70 rpm. The rods of blends were cooled in a water bath and then granulated.

The granulated blends were dried in a vacuum oven at 80°C for 10 h, and then injection molding was carried out with a barrel temperature of about 200°C to prepare Izod impact test and tensile test samples.

### Particle Size and Intensity by DLS Instrument

The hydrodynamic diameter and its distribution of the PB latex and PB-*g*-PS copolymer in aqueous media were characterized by ZetaPlus dynamic light scattering (DLS) detector (Brookhaven Instruments Corporation, Holtsville, NY, 27 mW laser, 657-nm incident beam, and 90° scattering angle). In this experiment, the PB latex and PB-*g*-PS particles were diluted to around 1 mg/mL concentration in an aqueous medium. Then the solutions including PB and PB-*g*-PS particles were put into the test cells at room temperature. After stabilizing for 24 h, the solution cells were measured by DLS at least five times.

### Mechanical Test

According to ASTM D256, the Izod-notched impact strength was determined with a XJU-22 impact tester at the maximum speed of 3.5 m/s. The tensile test was measured according to ASTM D638 using Shimadzu AGS-H 5 kN tensile tester at a crosshead speed of 50 mm/min. The test temperature was performed at 23°C ± 1°C, and at least five specimens were tested for each average value given.

### Morphology Observation

The morphologies of all samples were observed by using JEM-2000EX TEM. The specimens were cut to 50 nm in thickness using the microtome at the temperature of −100°C, and the ultrathin section was stained with $OsO_4$ evaporation for 8 h before observation.

## RESULTS AND DISCUSSION

### Grafting Polymerization

Core-shell PB-*g*-PS copolymers were synthesized via emulsion grafting polymerization by grafting styrene onto PB latex particles with AIBN as an oil-soluble initiator. The synthesized PB-*g*-PS copolymers were characterized by Fourier transform infrared (FTIR), and the FTIR spectra were shown in Figure 1. The PB-*g*-PS copolymers were extracted with acetone, and the wave number of PB-*g*-PS ranged from 1800 to 600 cm$^{-1}$. The FTIR spectrum of PB-*g*-PS was characterized by the presence of absorbance peaks attributed to the unsaturated carbon double bonds as follows: peaks at 1639, 1493, and 1452 cm$^{-1}$ for C=C stretching of the benzene ring, 910.3 and 965.2 cm$^{-1}$ for C—H bending of $CH_2$, 757.9 cm$^{-1}$ for C—H bending of the benzene ring, and 697.2 cm$^{-1}$ for corrugation vibration of the benzene ring. It was indicated that the grafting polymerization of PS onto PB molecule had taken place by using AIBN as an initiator.

The particle size distribution profile of PB and PB-*g*-PS copolymer was found to be 314.7 and 383.3 nm measured by DLS as shown in Figure 2, respectively. The narrow distribution in Figure 2 also indicates that PS had grafted onto PB rubber

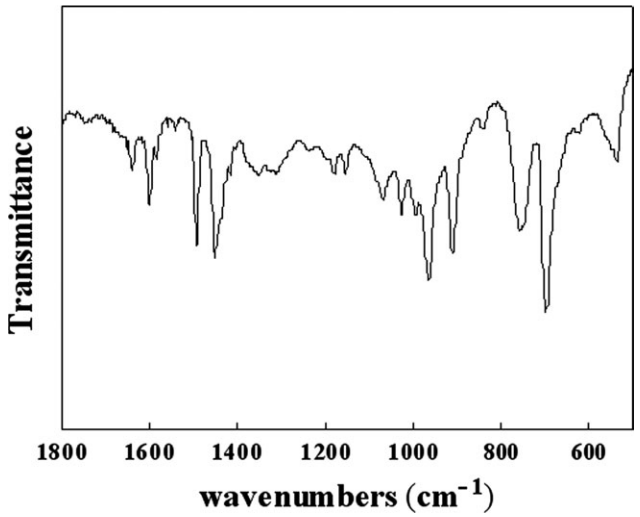


**Figure 1.** FTIR spectra of the PB-*g*-PS copolymer.

particles effectively. Moreover, the GD and GE of PB-*g*-PS were measured. The results showed that the GD and GE were 136% and 90.6%, respectively, which indicated that PS had grafted onto PB rubber particles efficiently.

### Mechanical Properties

The impact strength and tensile tests are the most widely used methods for measuring the toughness of materials. The notched Izod impact strength and yield tensile strength of HIPS/PS/PB-*g*-PS, PS/PB-*g*-PS, and HIPS were shown in Table I. First, we prepared a series of HIPS/PS/PB-*g*-PS with the same amount of HIPS, and the results showed that the impact strength increased and the tensile yield strength decreased with the increase of PB-*g*-PS in HIPS/PS/PB-*g*-PS. The PB rubber particles provide a soft phase in the blends, and the impact strength would increase with the rubber contents in materials. However, the increase of the amount of soft rubber particles also induced the decrease in the yielding strength. Also, we found from Table I that the impact strength of HIPS/PS/PB-*g*-PS (50/30/20) was 117.1 J $m^{-1}$, higher than the linear average value 109 J $m^{-1}$ between PS/PB-*g*-PS (60/40) and HIPS, which indicated that the toughness of PS could be enhanced through the combination of two kinds of rubber particles.

### Morphology and Dispersion of Rubber Particles

To observe the morphology of particles, the ultrathin sections of HIPS, PS/PB-*g*-PS, and HIPS/PS/PB-*g*-PS were measured by TEM. Figure 3 gave the transmission electron micrograph images of ultrathin sections of different samples. The section was stained with $OsO_4$, and the PB component could be observed as a black color. The PS shell from PB-*g*-PS was combined with the PS matrix, so that we cannot distinguish them clearly. As can be seen clearly from Figure 3(a), the interior of the particle contained the PS inclusion of PB-*g*-PS, and the particle size was about 1–2 $\mu$m. This kind of the rubber particle was called as "salami" rubber particle. In comparison with HIPS, the particle size and the PS inclusion zone of PB-*g*-PS, which were shown in Figure 3(b), were much smaller than that of HIPS. Moreover, the PB rubber particles were more likely to agglomeration in the PS matrix. From the TEM image of HIPS/PS/PB-*g*-PS in Figure 3(c), it can be seen clearly that in the sample, the rubber particles, including micrometer "salami" rubber particles and submicron-sized PB rubber particles, had a good dispersion in the matrix. As a result, the synergism between the two kinds of rubber particles could influence the toughness of PS.

### Deformation Mechanism

To explore the deformation mechanism of samples in the tensile test, we observed the macroscopic stress-whitening zone by TEM. The TEM images of stress-whitening zones for HIPS and PS/PB-*g*-PS were shown in Figure 4. From Figure 4(a), it was found that the interior of rubber particles contained a large number of inclusions of PS particles in HIPS. A large quantity of crazes was generated in the equator of rubber particles, and these crazes were very long. Crazes were initiated from one rubber particles and ended in another one. The results were consistent with the previous reports.[2,21] The crazes consisted of elongated voids and fibrils of highly oriented, aligned in the direction of the local maximum principal stress. It is well known that crazes are dilatational plasticity points and precursors to fracture and hence control the toughness of PS. For PS/PB-*g*-PS in Figure 4(b), it displayed a good deal of debonding cavitations due to the weak cohesive interaction between rubber particles and the matrix. Usually, the cavitations coming from

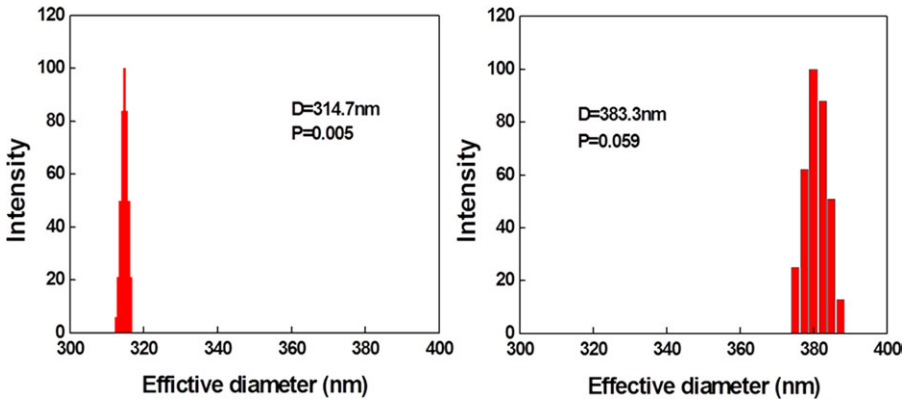


**Figure 2.** The size distribution of PB and PB-*g*-PS rubber particles measured by DLS: (a) PB; (b) PB-*g*-PS. [Color figure can be viewed in the online issue, which is available at wileyonlinelibrary.com.]

**Table I.** The Impact Strength and Yield Tensile Strength of HIPS/PS/PB-*g*-PS Blends

| Samples | HIPS | PS | PB-*g*-PS | Impact strength (J $m^{-1}$) | Yield tensile strength (MPa) |
|---|---|---|---|---|---|
| HIPS/PS/PB-*g*-PS (50/40/10) | 50 | 40 | 10 | 108.6 ± 3.8 | 27.8 ± 0.6 |
| HIPS/PS/PB-*g*-PS (50/30/20) | 50 | 30 | 20 | 117.1 ± 3.9 | 27.6 ± 0.6 |
| HIPS/PS/PB-*g*-PS (50/20/30) | 50 | 20 | 30 | 142.2 ± 4.3 | 26.2 ± 0.1 |
| HIPS/PS/PB-*g*-PS (50/10/40) | 50 | 10 | 40 | 165.9 ± 8.6 | 24.7 ± 1.3 |
| PS/PB-*g*-PS (60/40) | 0 | 60 | 40 | 146.4 ± 6.6 | 26.7 ± 0.2 |
| HIPS | 100 | 0 | 0 | 72.5 ± 1.2 | 27.5 ± 0.5 |

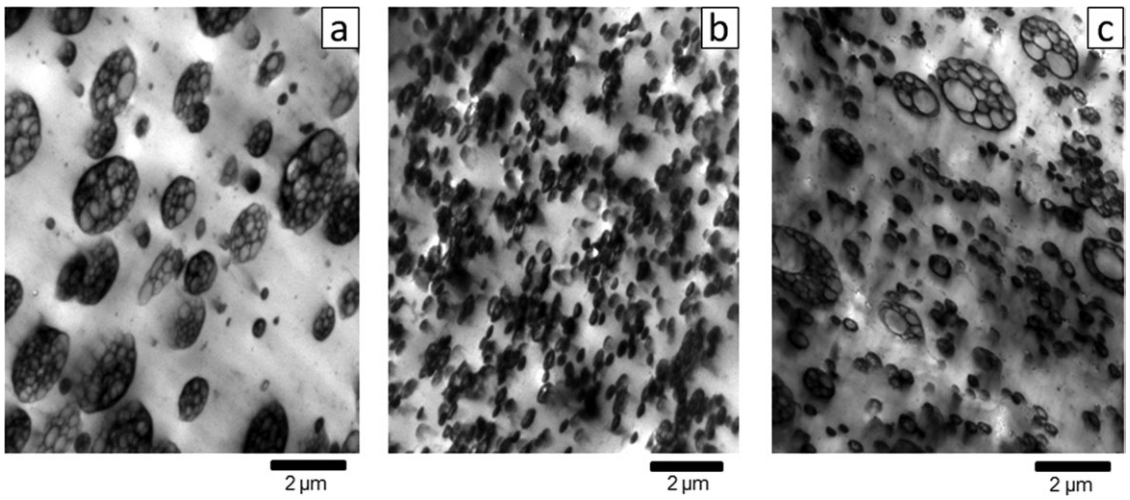


**Figure 3.** The transmission electron micrograph images of ultrathin sections of different samples: (a) HIPS; (b) PS/PB-*g*-PS; (c) HIPS/PS/PB-*g*-PS.

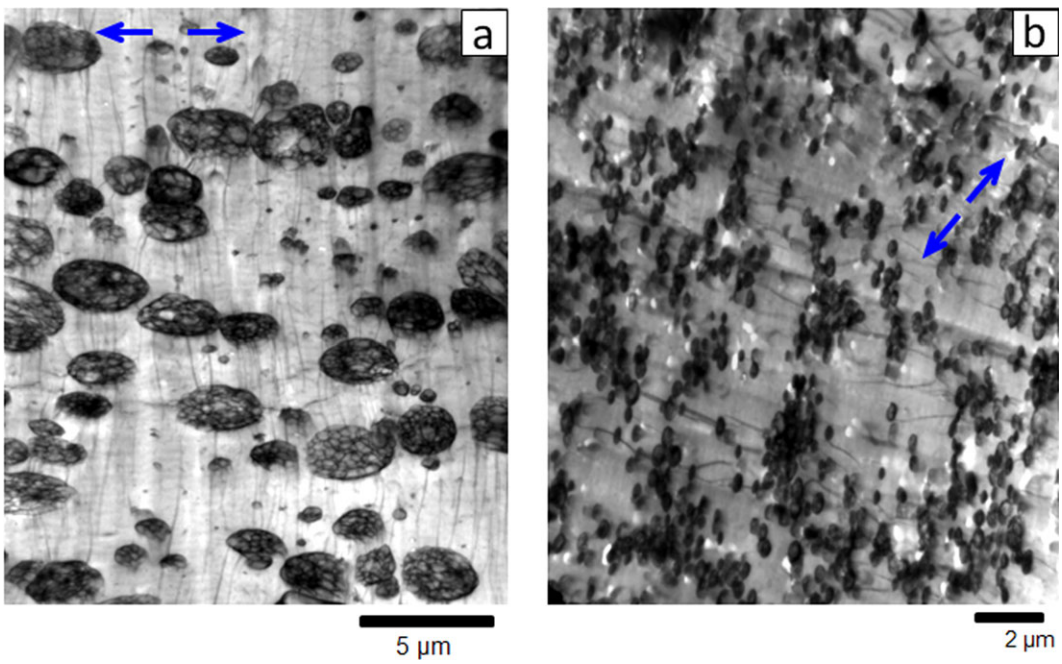


**Figure 4.** The TEM images of stress-whitening zone of blends in the tensile test: (a) HIPS; (b) PS/PB-*g*-PS. [Color figure can be viewed in the online issue, which is available at wileyonlinelibrary.com.]

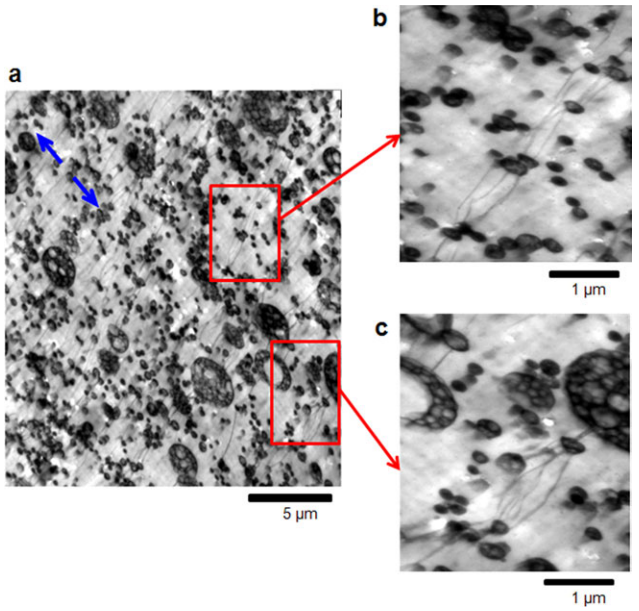


**Figure 5.** The TEM images of stress-whitening zone of HIPS/PS/PB-*g*-PS in the tensile test. [Color figure can be viewed in the online issue, which is available at wileyonlinelibrary.com.]

small rubber particles toughening plastics were considered as a deformation mechanism that the shear yielding following cavitations could improve toughness of PS, similar to our previous reported work.[14] And some short crazes were also observed to be initiated from the agglomeration rubber particles (particle zones) and ended to the surrounding rubber particles [Figure 4(b)]. In general, small particles tend to produce cavitation and shear yielding, whereas larger particles (or particle zones) are more effective for initiating crazing when external force exerts on the materials.[22–24] Both toughening processes can absorb much energy and contribute to the toughness of PS. The results suggested that the dominant deformation mechanism of PS/PB-*g*-PS blend was crazes and cavitations.

For HIPS/PS/PB-*g*-PS, the TEM image of stress-whitening zone was shown in Figure 5. The TEM image of HIPS/PS/PB-*g*-PS indicated that a large number of crazes generated in the direction nearly perpendicular to the loading and extended to neighboring rubber particles parallel to the equatorial plane in a bridge-like manner. Especially, due to the synergism between two kinds of submicrometer rubber particles and micrometer salami structure particles, the stress fields of rubber particles in the PS matrix were overlapped, and the stress-induced craze was decreased. As a result, a large number of crazes were initiated from the rubber particles, including not only the salami structure rubber particles but also the submicrometer particles. Moreover, we selected two typical areas from the stress-whitening zone, and the large-scale images were shown in Figure 5(b,c). As indicated by the arrows, the crazes can be initiated from small rubber particles and extended to neighboring small ones. Or crazes can be initiated from large salami rubber particles, go through small rubber particles, which could be called "craze-bridge" particles, and end to other neighboring small ones, preventing excessively crazing to form cracks and absorbing much energy to significantly enhance the toughness of materials.

## CONCLUSIONS

The submicrometer core-shell PB-*g*-PS copolymers were synthesized by emulsion grafting polymerization by grafting styrene onto PB latex with AIBN as an initiator. The FTIR spectroscopic analysis confirmed that PS had been successfully grafted onto the PB rubber particles. Then, the HIPS/PS/PB-*g*-PS blends were prepared by blending PB-*g*-PS copolymers with HIPS and PS. The notched impact strength of HIPS/PS/PB-*g*-PS was higher than expected as a linear average of HIPS and PS/PB-*g*-PS due to synergism of micrometer salami rubber particles and submicron-sized core-shell PB-*g*-PS particles. The stress-whitening zone of HIPS/PS/PB-*g*-PS in a tensile condition was observed by TEM. Crazes can be initiated from small rubber particles and ended to neighboring small ones. Moreover, crazes can be initiated from large salami rubber particles, go through small rubber particles, which could be called "craze-bridge" rubber particles, and end to other neighboring small ones, preventing excessively crazing to be form cracks and absorbing much energy to significantly enhance the toughness of materials.

## ACKNOWLEDGMENTS

This research was financially supported by a grant from National Natural Science Foundation of China (NSFC; No. 51073027, No. 51003007, No. 51103014, and No. 51173020) and Scientific and Technological Developing Plan Project of Jilin Province (No. 20110340).

## REFERENCES

1. Rovere, J.; Correa, C. A.; Grassi, V. G.; Pizzl, M. F. D. *Polym. Sci.* **2008**, *18*, 12.
2. Sharma, R.; Socrate, S. *Polymer* **2009**, *50*, 3386.
3. Coutinho, F. M. B.; Costa, M. P. M.; Guimaraes, M. J. O. C.; Soares, B. G. *J. Appl. Polym. Sci.* **2008**, *108*, 406.
4. Quan, Z.; Wang, H.; Zhao, H.; Lin, S. *Polym. Mater. Sci. Eng.* **2009**, *25*, 105.
5. Quan, Z.; Wang, H.; Zhao, H.; Lin, S. *Polym. Mater. Sci. Eng.* **2010**, *26*, 89.
6. Silberberg, J.; Han, C. D. *J. Appl. Polym. Sci.* **1978**, *22*, 599.
7. Donald, A. M.; Kramer, E. J. *J. Mater. Sci.* **1982**, *17*, 2351.
8. Piorkowska, E.; Argon, A. S.; Cohen, R. E. *Macromolecules* **1990**, *23*, 3838.
9. Okamoto, Y.; Miyagi, H.; Kakugo, M. *Macromolecules* **1991**, *24*, 5639.
10. Okamoto, Y.; Miyagi, H.; Mitsui, S. *Macromolecules* **1993**, *26*, 6547.
11. Maestrini, C.; Monti, L.; Kausch, H. H. *Polymer* **1996**, *37*, 1607.
12. Bucknall, C. B. *J. Microsc.* **2001**, *201*, 221.
13. Perkins, W. G. *Polym. Eng. Sci.* **1999**, *39*, 2445.

14. Gao, G. H.; Zhang, J. S.; Yang, H. D.; Zhou, C.; Zhang, H. X. *Polym. Int.* **2006**, *55*, 1215.
15. Gao, G. H.; Yang, H. D.; Zhou, C.; Zhang, H. X. *J. Appl. Polym. Sci.* **2007**, *103*, 738.
16. Cohen, R. E.; Bates, F. S. *J. Polym. Sci. Polym. Phys.* **1980**, *18*, 2143.
17. Huang, N. J.; Sundberg, D. C. *J. Polym. Sci. Polym. Chem.* **1995**, *33*, 2533.
18. Huang, N. J.; Sunberg, D. C. *J. Polym. Sci. Polym. Chem.* **1995**, *33*, 2551.
19. Huang, N. J.; Sundberg, D. C. *J. Polym. Sci. Polym. Chem.* **1995**, *33*, 2571.
20. Capek, I. *Colloid Interf. Sci.* **2001**, *91*, 295.
21. Bucknall, C. B.; Smith, R. R. *Polymer* **1965**, *6*, 437.
22. Ramsteiner, F.; Heckmann, W.; McKee, G. E.; Breulmann, M. *Polymer* **2002**, *43*, 5995.
23. Alfarraj, A.; Nauman, E. B. *Polymer* **2004**, *45*, 8435.
24. Hu, Y.; Jia, Z.; Li, Y.; Chang, L.; Wang, Y. *Mater. Sci. Eng. A* **2011**, *528*, 6667.